Ultrasonics - Sonochemistry 70 (2021) 105327

Contents lists available at ScienceDirect

Ultrasonics - Sonochemistry

journal homepage: www.elsevier.com/locate/ultson

Enhanced adsorption of Congo red using chitin suspension after sonoenzymolysis

Furong Hou[a], Danli Wang[a], Xiaobin Ma[a], Lihua Fan[a], Tian Ding[a,c], Xingqian Ye[a,b,c], Donghong Liu[a,b,c,*]

[a] College of Biosystems Engineering and Food Science, Zhejiang University, Hangzhou 310058, China
[b] Fuli Institute of Food Science, Zhejiang University, Hangzhou 310058, China
[c] Zhejiang Key Laboratory for Agro-Food Processing, Zhejiang R&D Center for Food Technology and Equipment, Hangzhou 310058, China

ARTICLE INFO

Keywords:
Chitin suspension
Sonoenzymolysis
Congo red
Adsorption properties

ABSTRACT

In the present work, chitin suspensions after enzymolysis and sonoenzymolysis were taken as adsorbents to evaluate the adsorption properties of Congo red (CR) dyes. Compared with untreated chitin suspension, the CR adsorption performance was significantly improved after enzymolysis and even more after sonoenzymolysis. According to different adsorption kinetic and isotherm models, Langmuir isotherm and the pseudo-second order model were more reliable to describe the adsorption process of CR onto different chitin samples and demonstrated a monolayer and favorable physisorption process. What's more, negative values of ΔG (Gibbs free energy change) and the shifts to higher negative values with the temperature increasing from adsorption thermodynamic study proved a spontaneous CR adsorption process. The structural characterization before and after adsorption further verified the physical adsorption between chitin and CR, and a larger specific area and higher porosity of chitin suspension was obtained after sonoenzymolysis with more available active sites.

1. Introduction

Chitin, the second most abundant natural polysaccharide following to cellulose, is one of the most fascinating sustainable polymers coming from various marine creatures, such as shrimp and crab shells [1]. While most of them are regarded as the wastes and discarded in nature, causing serious resource wastes and environmental pollutions [2]. Coupled with the highly crystalline and low solubility of chitin, it further limits its application. Therefore, many studies were focused on exploring potential ways to reduce the pollution and obtain value added chitin products. For example, GlcNAc and $(GlcNAc)_2$ were obtained by enzymatic degradation from pretreated grinding chitin shells, which could be used as skin moisturizers and antimicrobial agents [3]. Instant catapult steam explosion treatment could lower chitin crystallinities and increase surface areas and pore volumes, this was benefited to dye adsorption by increasing the binding surface area [4,5].

Colored compounds are widely used in textile and dye industries as esthetic materials, while the direct release of effluents without treatment is one of the main sources of water pollution, in which dyes into the natural environment will led to life-threatening diseases for the creatures living in the world [6]. Congo red (CR), as one of the anionic direct diazo dyes, is possessed with the physicochemical, thermal and optical stability owing to the aromatic structure [7], which are usually used to evaluate the specific surface areas of cellulosic substrates [5]. However, it's precisely because of the stability, making it difficult to be degraded. The presence of these residual dyes in effluents could contaminate the environment and do harm to organisms and human health even at low concentrations [8]. Therefore, the removal of the dye has attracted much attention of many researchers. Adsorption is regarded as one of the most promising decontamination techniques due to its simple operation, low cost as well as the wide source of adsorbents [9].

Recently, chitin-based products have been found that it could be as an adsorbent for dye removal. It was reported that α-chitin after acidic treatment and ultrasonication could adsorb organic dye easily from the aqueous solution, which was ascribed to its lowered crystallinity index and increased specific surface area [10]. Chitin–AC (activated carbon) exhibited a higher adsorption capacity of cephalexin antibiotic compared with other ACs from agricultural and industrial origins, resulted from the featured functional multi-sites of antibiotic adsorption [11]. What's more, fluoride could be removed by modified chitin with bimetallic oxide powder (Ca–Zn @Chitin). Compared with the original Ca–Zn and chitin, this composite was thermally more stable and porous, which enhanced the adsorption capacity through the surface hydroxyl groups, electrostatic and ion-dipole interaction between fluoride and

* Corresponding author at: College of Biosystems Engineering and Food Science, Zhejiang University, 866 Yuhangtang Rd., Hangzhou 310058, China.
E-mail addresses: danliwang@zju.edu.cn (D. Wang), xbma@zju.edu.cn (X. Ma), psu@zju.edu.cn (X. Ye), dhliu@zju.edu.cn (D. Liu).

https://doi.org/10.1016/j.ultsonch.2020.105327
Received 1 July 2020; Received in revised form 5 August 2020; Accepted 27 August 2020
Available online 01 September 2020
1350-4177/

calcium [12].

Nowadays, some studies have been shown that enzymolysis could increase the adsorption capacities of some adsorbents by increasing the specific surface area, pore size and volume. Guo [13] has found that the adsorption capacity of glycosyl-transferase/α-amylase/ glucoamylase treated starches increased by about 7–21 folds compared to the original starch. Additionally, Zhang [14] has proved that adsorption efficiency was exponential to hydrolytic production of ultrafine grinding pretreated corn stover. According to many researchers, ultrasound could significantly enhance the enzymolysis process due to its cavitation effect, generating cavitation bubbles and collapse into high-energy jets by activating the enzyme, breaking up the biopolymer and increasing the mass transfer process [15–17]. According to our previous work [18], it had proved that ultrasound could enhance the enzymolysis of chitin, and led to the decrease of crystalline index with the potential of increasing adsorption capaicty. During the enzymatic process, the present of ultrasound could deeply destroy the fiber structure of chitin and accelerate high-velocity interparticle collisions between enzyme and substrate due to its cavitation effect, leading to a significantly high enzymatic efficiency [19]. Although it has been reported that chitin is characterized with the power to adsorb dyes [5,10], it's meaningful to measure adsorption properties of chitin after enzymolysis and sonoenzymolysis in order to provide a more efficient material to decontaminate dyes from industrial wastewater. Therefore, in the present study, different chitin samples obtained after enzymolysis and sonoenzymolysis were used as adsorbent to evaluated the adsorption properties for the removal of CR dyes. Varieties of adsorption isotherms, kinetics and thermodynamics were applied to investigate the adsorption characteristics. Furthermore, the structural properties before and after adsorption were examined to illustrate the potential mechanism of adsorption.

2. Methods and materials

2.1. Materials

Chitin and chitinase were purchased from Sigma-Aldrich (Shanghai, China) and without any further purification for use, chitin was from shrimp shells and chitinase was from *Streptomyces griseus* (EC3.2.1.14). All of other reagents were purchased from Sinopharm Co., Ltd. with analytical grade (Shanghai, China).

2.2. Preparation of chitin samples

The chitin samples were included the chitin suspension (CS), enzymolysis of chitin suspension (CSE) and sonoenzymolysis of chitin suspension (CSSE). The CS was prepared as the method described in previous study [18], the CES was obtained after the enzymolysis of chitinase (0.1 mg/mL, pH 6) for 20 min at 50 °C, and the CSSE was obtained after the sonoenzymolysis (frequency of 22 kHz, ultrasonic intensity of 25 W/mL) for 20 min at 50 °C.

The reason to choose the above conditions to get the CSE and CSSE is that the highest enzymatic efficiency could be obtained under that treatment condition according to our previous study [18].

2.3. Adsorption experiments

Firstly, the chitin samples were dialyzed (tube MD 34) for 2 days against the phosphate buffer. In order to test the ability of chitin samples to remove the CR from aqueous solution, a batch of adsorption experiments were conducted in a reaction mixture of 1 mL (1–5 mg/ml) of chitin samples and 4 mL of CR (100–300 mg/L) at 20–50 °C under magnetic stirring. After 10 to 180 min, the samples were centrifuged for 10 min to obtain the supernatant, and measured the absorbance at 488 nm with a UV-2550 spectrophotometer. (SHIMADZU Co., Japan). The removal efficiency (R%) and adsorption capacity (Q_e, mg/g) were calculated by Eqs. (1) and (2), respectively.

$$R(\%) = \frac{C_0 - C_e}{C_0} \times 100\% \tag{1}$$

$$Q_e = \frac{(C_0 - C_e)}{m} \times V \tag{2}$$

where C_0 and C_e are the initial and equilibrium concentrations of CR (mg/L) respectively, m is the weight of the chitin samples (g) and V is the volume of the CR (L) [19].

2.4. Adsorption isotherms of CR with different chitin samples

The adsorption isotherms indicate the relationship between the adsorption saturation and the adsorption concentration with specific temperature, which could reflect the adsorption ability of chitin and help to reveal the adsorption process mechanism [20].

2.4.1. Langmuir isotherm model

The Langmuir isotherm, a semi-empirical model, is hypothesized as a monolayer adsorption phenomenon without interaction between adsorbed neighboring molecules on a homogeneous surface [20].

$$\frac{C_e}{Q_e} = \frac{1}{K_L Q_m} + \frac{C_e}{Q_m} \tag{3}$$

where Q_m is the Langmuir maximum adsorption of the CR (mg/g) and K_L is the Langmuir constant (L/mg), Q_e and C_e are mentioned above.

R_L is a basic characteristic parameter for evaluating the Langmuir isotherm adsorption process:

$$R_L = \frac{1}{1 + K_L C_0} \tag{4}$$

where b and C_0 are the same as mentioned above. The shapes for $R_L = 0$, $0 < R_L < 1$, $R_L = 1$ and $R_L > 1$ are represented as irreversible, favorable, linear and unfavorable adsorption, respectively.

2.4.2. Freundlich isotherm model

The Freundlich isotherm, an empirical model, could be used to describe both monolayer and multilayer adsorption because of its effectiveness on heterogeneous surfaces [21].

$$\lg Q_e = \lg K_F + \frac{\lg C_e}{n} \tag{5}$$

where n is an indication of the adsorption favorability of different chitin samples and K_F is the adsorption capacity. Generally, the shapes of the isotherms for $0 < 1/n < 1$, $1/n = 1$ and $1/n > 1$ are favorable, linear and unfavorable adsorption, respectively.

2.4.3. Dubinin–Radushkevich (DR) model

D-R model is usually used to distinguish whether the adsorption is physical or chemical adsorption with a Gaussian energy distribution on a heterogeneous surface, which could be evaluated by the mean free energy E (kJ/mol). The process is physisorption if $E < 8$ kJ/mol, while is chemisorption if $8 < E < 16$ kJ/mol [22].

$$\ln Q_e = \ln Q_s - K_{ad}\varepsilon^2 \tag{6}$$

$$\varepsilon = RT\ln\left(1 + \frac{1}{C_e}\right) \tag{7}$$

$$E = \frac{1000}{\sqrt{2K_{ad}}} \tag{8}$$

where K_{ad} is D-R isotherm constant (mol^2/kJ^2).

2.5. Adsorption kinetics of CR with different chitin samples

Adsorption kinetics is to study the rate control of the process when

the adsorbent's adsorption of the adsorbate reaches to the equilibrium, including the spread of the adsorbate to the adsorbent and the adsorption of the adsorbate on the adsorbent's surface. It's dependent on the physical and chemical characteristics of the adsorbent (e.g. the existence of active sites of the adsorbent) as well as the favorability of the adsorbate to access to the sorbent's surface [23]. In this adsorption process, pseudo-first order, pseudo-second order and Weber-Morris kinetic models were used to describe the adsorption behavior of CR from aqueous solution on to the chitin.

2.5.1. Pseudo-first-order kinetic model

The pseudo-first-order kinetic model refers to a linear relationship between the reaction rate and the concentration of a reactant, based on the assumption that adsorption is controlled by a diffusion step [20].

$$\lg(Q_e\text{-}Q_t)=\lg Q_e\text{-}K_1 t \tag{9}$$

where K_1 (g/mg/min) is the rate constant of adsorption and Q_t is the adsorption capacity (mg/g) at time t, Q_e is the same as mentioned above.

2.5.2. Pseudo-second-order kinetic model

The pseudo-second-order model reveals that the rate of sorption depends linearly on the square of the unoccupied sites, based on the assumption of following a second-order mechanism [24].

$$\frac{t}{Q_t}=\frac{1}{K_2 Q_e^2}+\frac{1}{Q_e}t \tag{10}$$

where K_2 is the rate constant of the pseudo-second-order model (g/mg/min), Q_e and Q_t are the same as mentioned above.

2.5.3. Weber-Morris model

The Weber–Morris is a model that is used to explain intra-particle diffusion [25]:

$$Q_t=K_d t^{1/2}+C \tag{11}$$

where K_d (mg/g $min^{1/2}$) is the intra-particle diffusion rate constant, and C (mg/g) is an indicator that can reflect the boundary layer thickness [6].

2.6. Adsorption thermodynamic parameters of CR with different chitin samples

In order to understand the adsorption nature of CR onto different chitin samples, the basic thermodynamic characteristics of entropy change (ΔS), enthalpy change (ΔE) and Gibbs free energy change (ΔG) were determined during the adsorption according to Eqs. (13) and (14) [26]:

$$\ln(K_c) = -\frac{\Delta G}{RT} \tag{12}$$

$$\Delta G = \Delta H - T\Delta S \tag{13}$$

$$\ln(K_c) = -\frac{\Delta H}{RT} + \frac{\Delta S}{R} \tag{14}$$

where R is the gas constant (8.314 J/mol/K) and T is the degree Kelvin. K_c is the ratio of C_{Ae} (the concentration of CR adsorbed on the adsorbent) to C_e (the equilibrium concentration of CR in solution).

2.7. Goodness of model fit

The fit goodness of the applied isotherm models to the experimental data could be reflected through these following parameters: the correlation coefficient (R^2) after the linear regression, the composite fractional error function (CFEF) and the chi-square statistic (χ^2) [25]:

$$\mathrm{CFEF} = \sum_{n=1}^{n}\left[\frac{(Q_{e,exp}-Q_{e,cal})^2}{Q_{e,exp}}\right] \tag{15}$$

$$\chi^2 = \sum_{n=1}^{n}\left[\frac{(Q_{e,exp}-Q_{e,cal})^2}{Q_{e,cal}}\right] \tag{16}$$

where n is the number of experimental samples, $Q_{e,cal}$ (mg/g) and $Q_{e,exp}$ (mg/g) are the model calculated and experimental values of adsorption capacity, respectively.

2.8. Characterization of chitin samples

2.8.1. Fourier transform infrared spectroscopy (FTIR)

The functional groups were measured by a Nicolet 5700 FTIR spectrometer (Thermo Fisher Scientific, MA, USA), at a resolution of 4 cm^{-1} with a wavenumber range of 4000 to 400 cm^{-1}. The spectra were recorded after a total of 32 scans with three repeated measurements with the samples preparing into KBr pellets.

2.8.2. Surface area

The specific surface areas and pore volumes of different chitin samples were measured by the Autosorb-1-C (Quantachrome Ins, USA) from the N_2 adsorption-desorption isotherms at −196 °C (liquid nitrogen temperature), and were calculated by Brunauer-Emmett-Teller (BET) and Barrett-Joyner-Halenda (BJH) method [12].

2.8.3. X-ray photoelectron spectroscope (XPS)

The XPS spectra (ESCALAB 250Xi, Thermo Scientific, CA, USA) were obtained to determine the functional groups of the different chitin samples. The contents of C, O, N, S and Na were analyzed with an Al Kα X-ray ($h\nu$ = 1486.6 eV) excitation source, each of detected element were obtained after 12 scans. These spectra were calibrated to C (1s) signal at the binding energy of 284.80 eV.

2.8.4. UV-absorbance measurement

The absorbance of CR solutions before and after adsorption by different chitin samples were measured, carrying out by a spectrophotometer (UV-2550, SHIMADZU Co., Japan) ranging from 200 to 800 nm.

2.9. Statistical analysis

All results were presented as mean ± standard deviation after three repeated times. Statistical analysis was performed by SPSS 18.0 (SPSS Inc., Chicago, IL, USA) and Origin Software 8.5 (Origin Lab Corp., MA, USA).

3. Results and discussions

3.1. Effect of CR initial concentration and adsorbent dosage

3.1.1. Effect of CR initial concentration

The effect of initial concentration of CR to the adsorption by different chitin samples was shown in Fig. 1A. With the increase of CR concentration varied from 100 to 300 mg/L, Q_e of different chitin samples was increased. This was due to the higher the CR concentration (before the saturation of active sites), the more available to be adsorbed on the surface area of chitin [27], by overcoming the mass transfer resistance and increasing the driving force between the soluble phase and the adsorbent. What's more, the adsorption process was also enhanced due to the increasing number of collisions between CR and adsorbent [28]. The removal efficiency was decreased with the increase of initial CR concentration. With the adsorption sites got saturated, the percentage removal of CR would not increase when the CR concentration increased, attributing to the certain amount of available active sites on the surface area to the dye molecules [29], thereby exhibiting a

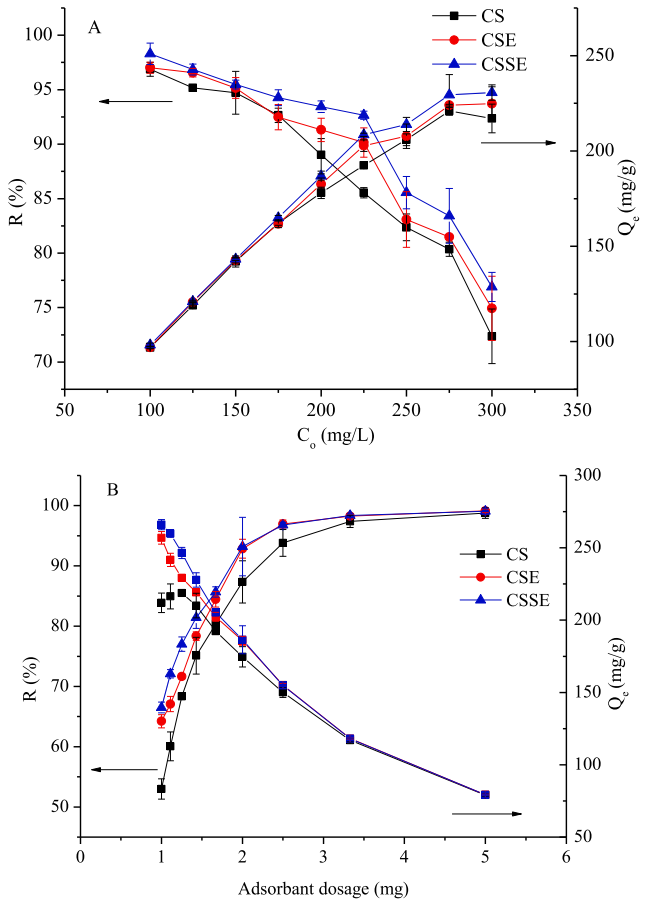

Fig. 1. Effect of CR initial concentration (A) and adsorbent dosage (B) to the adsorption of CR (20 °C, pH 6, 60 min).

negative effect. Further it can be seen that CSSE and CSE demonstrating a higher adsorption capacity than CS, indicating more active sites were generated during enzymolysis and even more in sonoenzymolysis. It's assuming that amorphous region could generate during enzymolysis, increasing the pore number and size on the specific surface area of chitin, resulting in the increment in CR adsorption [13]. Ultrasound treatment could accelerate this process due to its cavitation effect, adding the potential by decreasing the granularity and creating smoother surfaces, both of which led to a higher adsorption capacity of the CSSE than of CSE and CS [30].

3.1.2. Effect of adsorbent dosage

The effect of adsorbent dosage on CR (1 to 5 mg) removal efficiency and adsorption capacity were studied (Fig. 1B). The results showed that the removal percentage of CR was considerably increased with increasing amount of the adsorbents in the range of 1–2 mg, where more surface area containing adsorption sites was obtainable for adsorption and thereby making easier penetration of CR to adsorption sites [31]. While over the adsorbent dosage of 2 mg, the removal percentage reached to a constant value, because the available CR were almost fixed. Besides, according to Fig. 1B, adsorption capacity illustrated a decrease with the increase of adsorbent dosage, attributing to the increased unsaturated and overlapped adsorption sites during the process [32]. The same as Fig. 1A, the CSSE showed a higher adsorbent capacity compared with CSE and CS. This was ascribed to the increasing amount of the adsorption sites on adsorbent surfaces due to the loosen interchain structure during enzymolysis and sonoenzymolysis, which was discussed in the section 3.1.1.

3.2. Adsorption isotherms studies

The mathematical fittings of three isotherms were shown in Fig. 2 and isotherm fitting results were shown in Tables S1, Supporting Information.

Obviously, the Langmuir model was better than other isotherms to describe the adsorption of CR on chitin, based on the fact that the R^2 (correlation coefficients) of Langmuir isotherm was larger than that of Freundlich and D-R models. Furthermore, the lowest CFEF and χ^2 values suggested the most similarity as the calculated data to the experiment [25]. It also could be observed a favorable adsorption process through the R_L (from the Langmuir model) and 1/n (from Freundlich model) values, which were both in the range from 0 to 1. The Q_m (maximum monolayer adsorption capacity) calculated from the Langmuir isotherm was found to be increased with temperature from 293 K to 323 K, indicating higher temperature caused a swelling effect inside the internal structure of the chitin and benefited to the penetrating of CR in a naturally endothermic adsorption process [33]. All the R_L values calculated at a CR concentration of 100 mg/L were very close to the lower acceptable range (Tables S1), implying a high degree of irreversibility of the adsorption process [34]. In addition to the values of E (from D-R model) were lower than 8 kJ/mol, indicating the CR adsorption on different chitin samples were physisorption. Therefore, it could be concluded that the Langmuir isotherm was the best fitted to describe the adsorption of CR by chitin, exhibiting a monolayer and favorable physisorption process, involving the physical forces, like van der Waals force and hydrogen bonding [34].

The maximum adsorption capacity of CSSE as adsorbent for CR adsorption had a higher value (Q_m from the Langmuir model, K_F from the model and Q_s from the D-R model) and an excellent potential for the adsorption of CR dye compared with CS and CSE (Tables S1). More flexible polymer chains and active hydroxyl could be obtained in the case of sonoenzymolysis, indicating an enhanced adsorption capacity [14].

3.3. Adsorption kinetics

In order to examine the controlling mechanism of adsorption, three adsorption kinetic models were studied. The plots with various initial CR concentrations were shown in Fig. 3 and corresponding experimental results were listed in Tables S2.

It could be seen that the pseudo-second order model was more favorably to predict the adsorption process than the other two models due to the higher values of R^2 (all concentrations are above 0.999). Furthermore, a relatively good agreement between the experimental Q_e values and the calculated Q_e values could be obtained because of the low CFEF and χ^2 values (Tables S2). For the pseudo-second order kinetic model, the Q_e and K_2 values increased with the increase of initial CR concentration, which demonstrated the driving force between the solid and the liquid phase was enhanced at higher CR concentrations thereby decreasing the diffusion time of dye molecules onto the adsorbent binding sites [35].

Fig. 3 G, H I described the Weber-Morris model of CS, CSE and CSSE at different initial CR concentrations, where the fitting results were grouped into two steps. On the whole, a relatively fast adsorption stage (10–30 min) and a slow adsorption stage (30–180 min). In the first phase, the adsorption rate was fast, representing the external liquid film diffusion of the adsorbate to the adsorbent surface, while in the second phase, the adsorption rate gradually decreased resulted from the particle diffusion [25].

Moreover, additional fitting results were obtained that the two fitting linear steps did not pass through the origin ($C \neq 0$) at any concentrations, indicating that the adsorption of CR was controlled not only by the liquid film diffusion but also by the particle diffusion [36]. With the initial CR concentration increasing, for the same linear section, the values of C were increased, implying an enhanced boundary

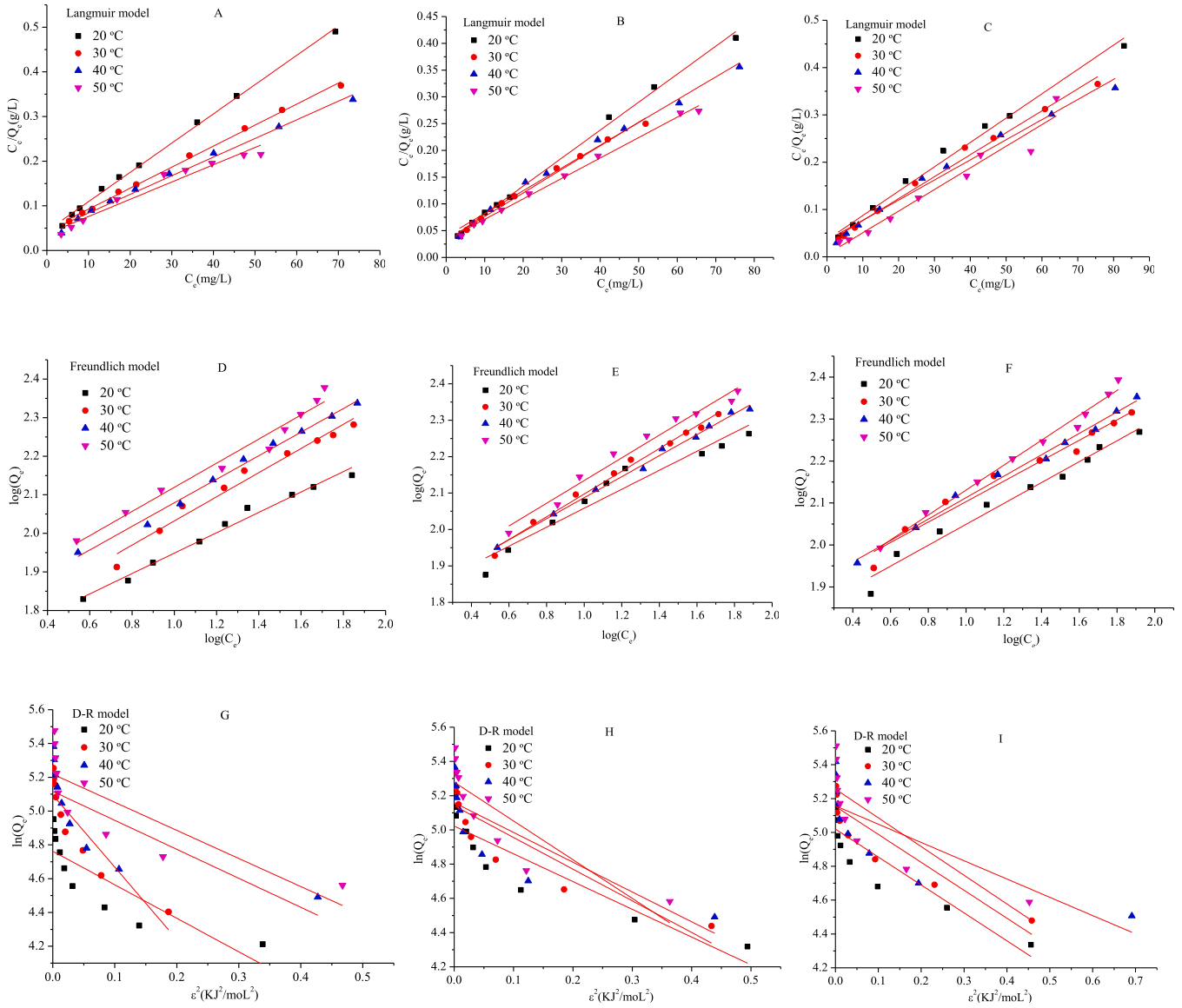

Fig. 2. Isotherms of the adsorption of CR on different chitin samples through Langmuir, Freundlich, and D-R model (CS: A, D, G; CSE: B, E, H; CSSE: C, F, I).

layer effect as well as a greater participation of the liquid film diffusion at higher CR concentrations at the given time range [25]. On the basis of the results from the pseudo-second order model, CSSE had a higher value of Q_e compared with CSE and CS, implying an acceleration of adsorption induced by ultrasound.

Therefore, the pseudo-second order model could be more suitable to represent the adsorption process of CR onto different chitin samples, and CSSE exhibited a higher adsorption capacity.

3.4. Adsorption thermodynamic study

The corresponding thermodynamic parameters were listed in Table 1. It could be obtained that the CR adsorption process was endothermic naturally illustrated by the positive values of ΔH [37]. In addition, the values of ΔH were all less than 40 kJ/mol, implying the physical adsorption [38], which was agreed well with the results of D-R model (Fig. S1). The obtained positive values of ΔS displayed an affinity between the CR and chitin surface, and an increase of the randomness at the solid-solution interface with temperature rise during the adsorption process [26]. The adsorbed solvent molecules substituted the adsorbate, obtaining more translation entropy than the adsorbate molecules loss, thus making the randomness in the system universal. The negative values of ΔG at all temperatures and the shifts to higher negative values with increasing the temperature proved the spontaneous nature as well as the feasibility of the CR adsorption process with chitin [19].

3.5. Characterization of different chitin samples

3.5.1. FTIR analysis

The FT-IR spectra before and after adsorption in Fig. 4 were used to study the functional groups of CR and adsorbent. The peaks at 1177 and 1062 cm^{-1} were ascribed to the S═O stretching vibration of SO_3^{-2} groups of CR [39]. Moreover, the band at 1612 cm^{-1} and at 1347 cm^1 were associated to the presence of −N═N− stretching and the aromatic amine of CR, respectively [40]. As can be seen, these peaks mentioned above were only observed in CR, while not appeared in the chitin samples after adsorbing. What's more, the peak at1656 cm^{-1} in the amide I region was determined in all the chitin samples before and after adsorption, which was the confirmation of the existence of −C═O…H−N intra-sheet H-bonding [41], indicating that no obvious changes were found in the enzymolysis and sonoenzymolysis process. These results implied that the interaction between chitin and CR molecules was physical adsorption without breakage or formation of new bonds,

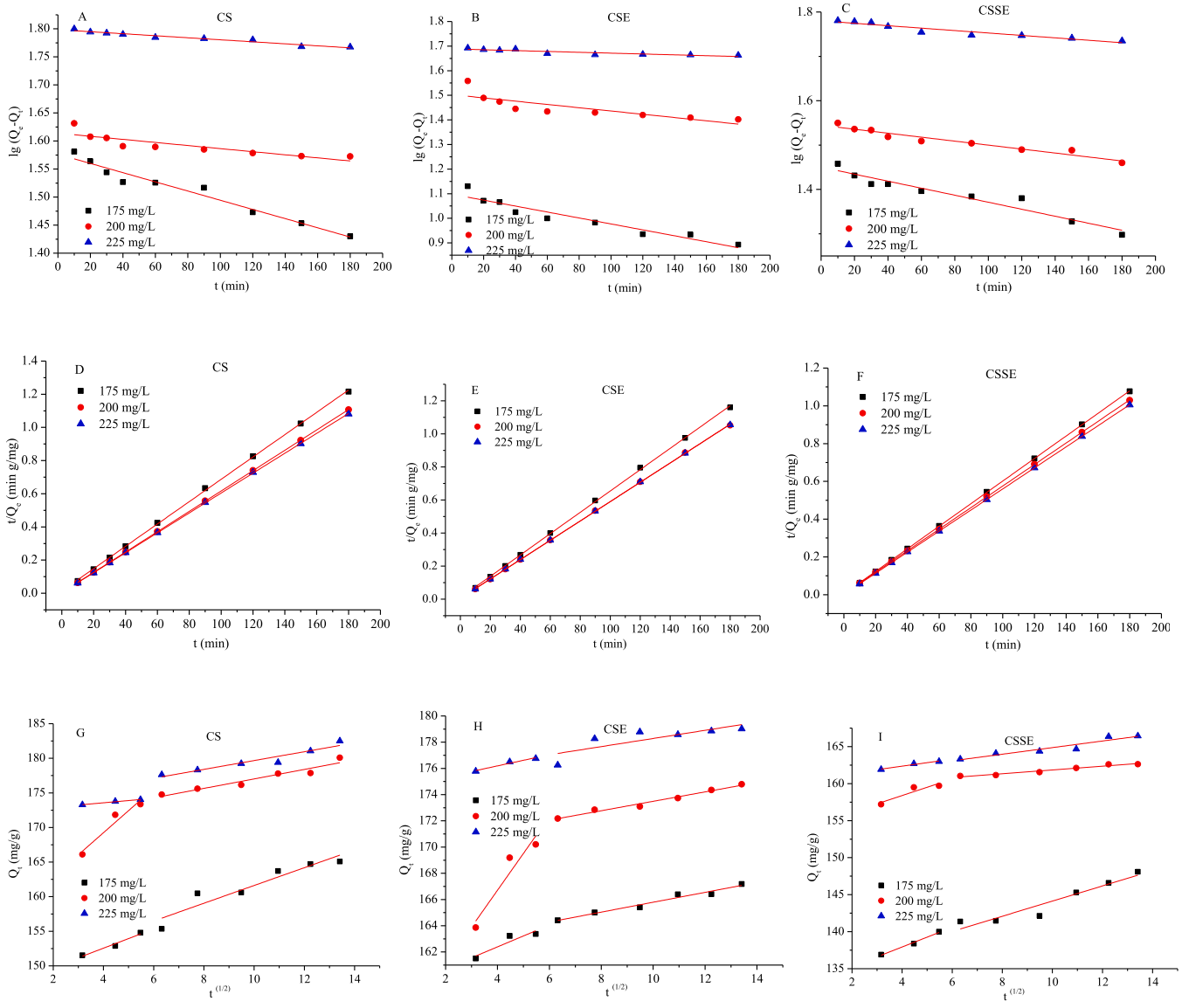

Fig. 3. Pseudo-first-order (CS:A, CSE:B, CSSE:C), pseudo-second-order (CS:D, CSE:E, CSSE:F) and Weber-Morris model (CS:G, CSE:H, CSSE:I) of CS, CSE and CSSE for the adsorption of CR (50 °C, pH 6, 60 min).

Table 1
Thermodynamic parameter for the adsorption of CR on different chitin samples.

	ΔH(kJ/mol)	ΔS(J/mol/K)	ΔG(kJ/mol)			
			293 K	303 K	313 K	323 K
CS	26.41	94.86	−27.77	−28.72	−29.67	−30.61
CSE	31.55	113.94	−33.35	−34.49	−35.63	−36.77
CSSE	33.12	119.81	−35.07	−36.27	−37.47	−38.67

which was consistent with the results of D-R model.

3.5.2. BET analysis

In order to determine the characteristic of the pores of chitin samples, the specific surface area, total pore volume and average pore diameter of different chitin samples were obtained through N_2 adsorption-desorption measurements and results were listed in Table 2. It showed that CS, CSE and CSSE were all in mesoporous structure, where all the average pore diameters were between 2 and 50 nm. It's reported that pore diameter could be divided into micropores ($d < 2$ nm), mesopores ($2 < d < 50$ nm) and macropores ($d > 50$ nm), and it's a basis of the total porosity [42]. Besides, the CSSE displayed a larger specific area and higher porosity, indicating that the presence of ultrasound treatment modified the porous structure of the adsorbent and made the active sites more available [43]. Therefore, it was benefited to accelerate the mass transfer and to obtain the equilibrium of adsorption reaction by improving the adsorption efficiency.

3.5.3. XPS analysis

In order to further reveal the effect of ultrasound and chitinase on the CS of adsorbing CR, XPS was applied to determine the existence of particular elements and the percentage of each content by exhibiting the binding energies (BE) and intensities [4]. The scan spectra of elements of O, C, N, S and Na were analyzed (Fig. 5), the existence of S 2p and Na 1s only on the surface of CR and the chitin samples after adsorption, indicating the presence of adsorption of CR. Meanwhile, the intensity of S and Na in CSSE was higher than CS and CSE, manifesting a strong adsorption of CSSE. The three marked 1, 2 and 3 peaks of chitin samples in C 1s spectra were assigned as C—C/C—H, C—O/C—N, and C═O/O—C—O groups [44]. Coupled with the other elemental scans, no significant changes of the BE of the elements before and after adsorption could be attributed to the weak interaction between CR and chitin

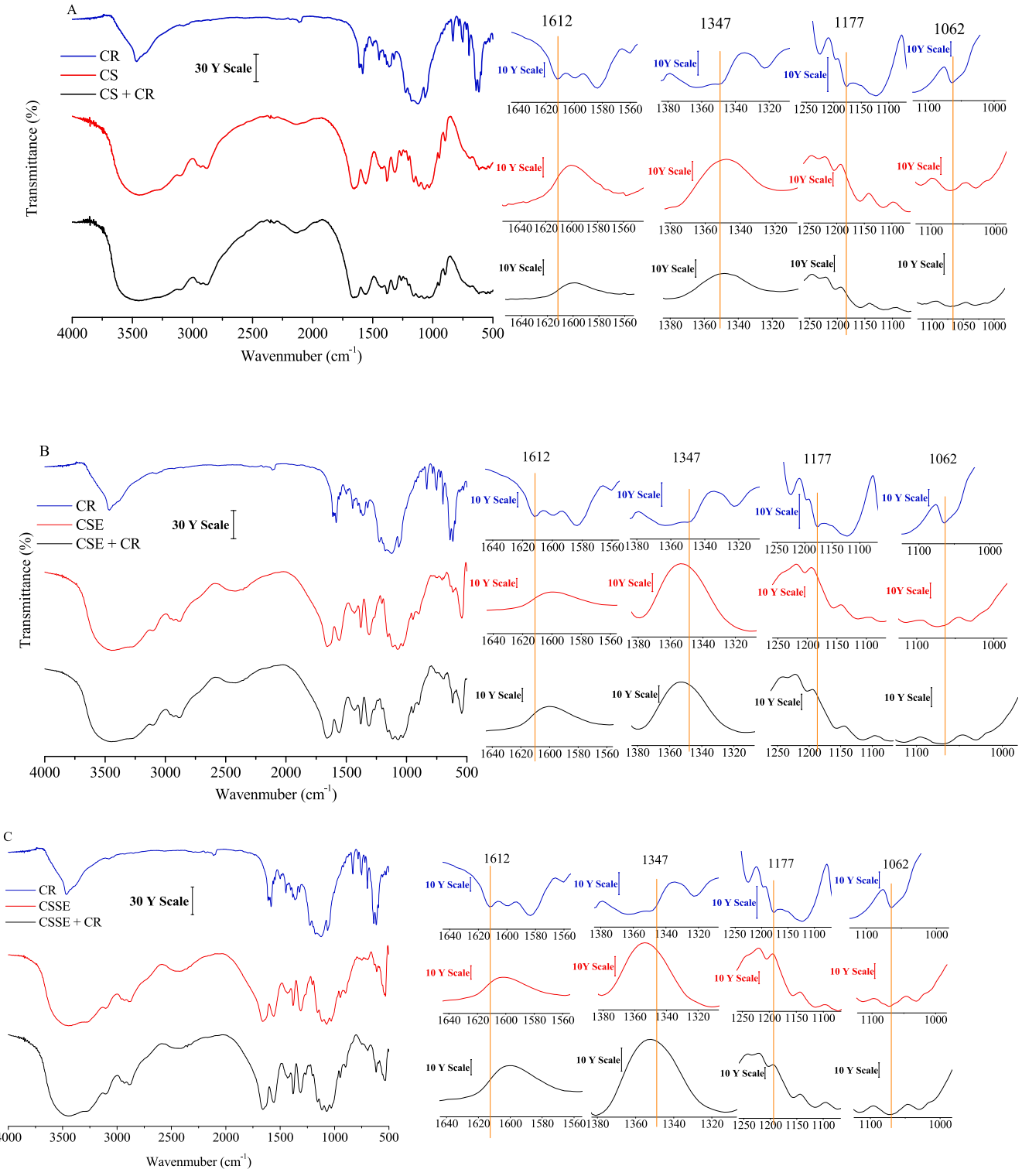

Fig. 4. FTIR spectra of different chitin samples before and after adsorption of CR.

samples, which resulted from the physical adsorption and was consistent with Chatterjee et al. [34]. The BE, full width half maximum (FWHM) and percentage content of elements of different chitin samples before and after adsorption were also listed (Tables S3).

3.5.4. UV-VIS

The UV–VIS spectra of CR (300 mg/L) solution before and after adsorption by different chitin samples for 60 min were presented and the corresponding photo was inset (Fig. 6). Typically, the maximum absorbance of CR was 488 nm, after addition of chitin the color of the dye solution became lighter and the absorbance intensity was decreased at all wavelength due to adsorption of CR. It was noticed that CSSE obtained the maximum adsorption compared with CS and CSE at the same reaction time and this effect before and after adsorption could be furtherly intuitively demonstrated by the inset digital photo. The enhanced adsorption of CSSE was due to the application of ultrasound,

Table 2
Specific surface area, total pore volume and average pore size of different chitin samples.

Sample	Specific surface area (m^2/g)	Average pore diameter (nm)	Total pore volume (cm^3/g)
CS	0.50	4.32	5.36×10^{-3}
CSE	0.97	5.17	6.79×10^{-3}
CSSE	1.22	9.33	8.53×10^{-3}

which was benefited to the increment of the interaction binding sites because of the increased specific surface area, total pore volume and average pore size volume, thereby increasing the diffusion and filling through mesoporous inter-channels [45]. This result was in agreement with the previous discussion in BET analysis.

4. Conclusions

Different chitin samples were applied for adsorption of CR. CSSE exhibited a relatively high adsorption capacity and removal efficiency, showing ultrasound was benefited to expose more active sites by increasing the specific surface area and by decreasing the granularity of chitin. Through the analysis of isotherms and kinetics, it could be concluded that the Langmuir as well as pseudo-second order kinetic model was the best fitted isotherm and kinetic model representing CR adsorption on CS. Combined with the results of the thermodynamics study, adsorption of CR by different chitin samples was a monolayer, endothermic and favorable physisorption process. The FTIR and XPS results of CS before and after adsorption were further confirm a natural physical adsorption could be occurred between chitin and CR. Besides, a larger specific area and higher porosity of CSSE were obtained according to the BET and UV–VIS analysis, indicating that ultrasound made CS porous thereby increasing the diffusion and filling. In a whole, these findings reveal the CR adsorption properties by different chitin samples, proving and providing that CSSE could be an excellent candidate for removal dyes from industrial wastewaters.

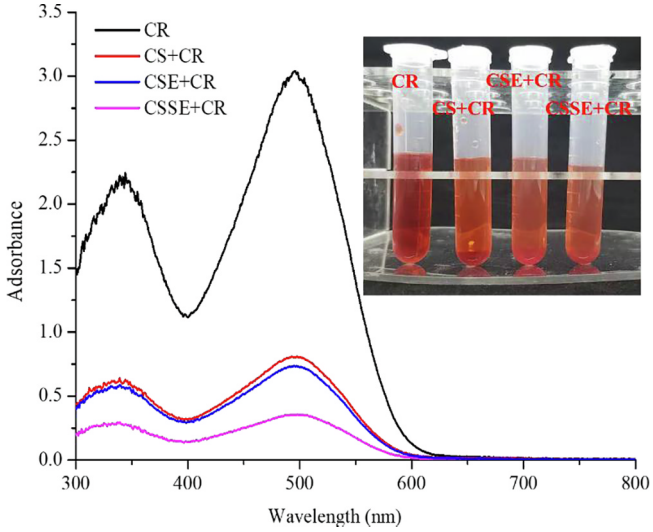

Fig. 6. UV–VIS spectra of different chitin samples before and after adsorption of CR.

CRediT authorship contribution statement

Furong Hou: Conceptualization, Methodology, Formal analysis, Writing - original draft. **Danli Wang:** Methodology, Software. **Xiaobin Ma:** Methodology, Investigation. **Lihua Fan:** Investigation. **Tian Ding:** Validation, Writing - review & editing. **Xingqian Ye:** Validation. **Donghong Liu:** Supervision, Project administration, Funding acquisition.

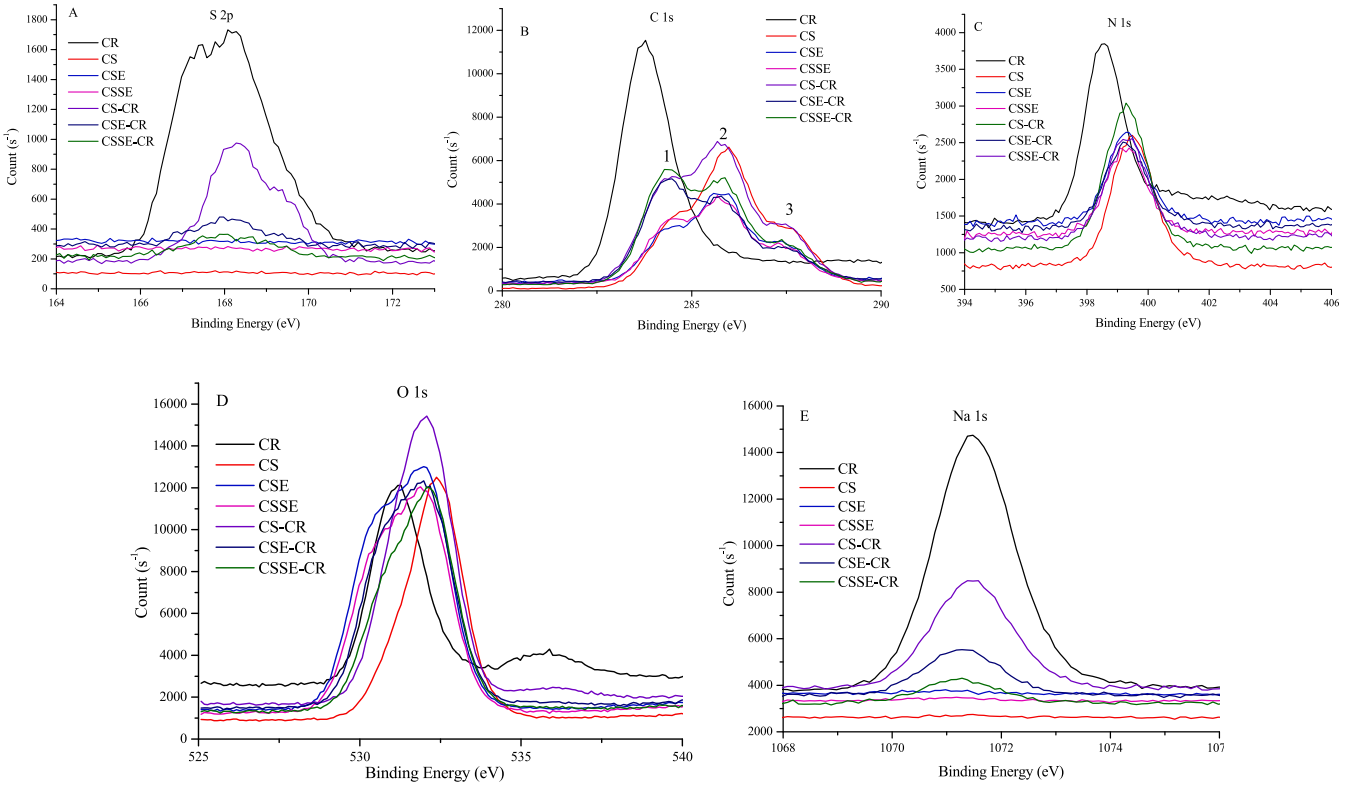

Fig. 5. XPS spectra of different chitin samples before and after adsorption of CR: (A) S 2p spectra; (B) C 1s; (C)N 1s; (D) O 1s; (E)Na 1s.

Declaration of Competing Interest

The authors declare that they have no known competing financial interests or personal relationships that could have appeared to influence the work reported in this paper.

Acknowledgements

This work was supported by the National Key Research and Development Program of China (2016YFD0400301), the Key Research and Development Program of Zhejiang Province (2017C02015) and National Natural Science Foundation of China (Grant No. 31901822).

Appendix A. Supplementary data

Supplementary data to this article can be found online at https://doi.org/10.1016/j.ultsonch.2020.105327.

References

[1] K.C. Li, R.G. Xing, S. Liu, P.C. Li, Advances in preparation, analysis and biological activities of single chitooligosaccharides, Carbohydr. Polym. 139 (2016) 178–190.
[2] G.G. Wei, A.L. Zhang, K.Q. Chen, P.K. Ouyang, Enzymatic production of N-acetyl-d-glucosamine from crayfish shell wastes pretreated via high pressure homogenization, Carbohydr. Polym. 171 (2017) 236–241.
[3] Y.S. Nakagawa, Y. Oyama, N. Kon, M. Nikaido, K. Tanno, J. Kogawa, S. Inomata, A. Masui, A. Yamamura, M. Kawaguchi, Y. Matahira, K. Totani, Development of innovative technologies to decrease the environmental burdens associated with using chitin as a biomass resource: Mechanochemical grinding and enzymatic degradation, Carbohydr. Polym. 83 (2011) 1843–1849.
[4] Z.Q. Tian, S.K. Wang, X.F. Hu, Z.M. Zhang, L. Liang, Crystalline reduction, surface area enlargement and pore generation of chitin by instant catapult steam explosion, Carbohydr. Polym. 200 (2018) 255–261.
[5] J.D. Goodrich, W.T. Winter, α-Chitin nanocrystals prepared from shrimp shells and their specific surface area measurement, Biomacromolecules 8 (2007) 252–257.
[6] J. Zolgharnein, S.D. Farahani, M. Bagtash, S. Amani, Application of a new metal-organic framework of $[Ni_2F_2(4,4'\text{-bipy})_2(H_2O)_2](VO_3)_2.8H_2O$ as an efficient adsorbent for removal of Congo red dye using experimental design optimization, Environ. Res. 182 (2020) 109054.
[7] G. Barman, A. Kumar, P. Khare, Removal of Congo red by carbonized low-cost adsorbents: process parameter optimization using a Taguchi experimental design, J. Chem. Eng. Data 56 (2011) 4102–4108.
[8] Z.C. Li, H. Hanafy, L. Zhang, L. Sellaoui, M.S. Netto, M.L.S. Oliveira, M.K. Seliem, G.L. Dotto, A. Bonilla-Petriciolet, Q. Li, Adsorption of congo red and methylene blue dyes on an ashitaba waste and a walnut shell-based activated carbon from aqueous solutions: Experiments, characterization and physical interpretations, Chem. Eng. J. 388 (2020) 124263.
[9] A. Yazidi, L. Sellaoui, G.L. Dotto, A. Bonilla-Petriciolet, A.C. Fröhlich, A.B. Lamine, Monolayer and multilayer adsorption of pharmaceuticals on activated carbon: application of advanced statistical physics models, J. Mol. Liq. 283 (2019) 276–286.
[10] E.H. Ablouh, R. Jalal, M. Rhazi, M. Taourirte, Surface modification of α-chitin using an acidic treatment followed by ultrasonication: Measurements of their sorption properties, Int. J. Biol. Macromol. 151 (2020) 492–498.
[11] W.A. Khanday, M.J. Ahmed, P.U. Okoye, E.H. Hummadi, B.H. Hameed, Single-step pyrolysis of phosphoric acid-activated chitin for efficient adsorption of cephalexin antibiotic, Bioresour. Technol. 280 (2019) 255–259.
[12] S. Nehra, S. Raghav, D. Kumar, Rod–shaped Ca–Zn@ Chitin composite forfluoride removal studies byadsorption and statistical experiments, Environ. Nanotechnol., Monit. & Manage. 12 (2019) 100264.
[13] L. Guo, J.H. Li, H. Li, Y. Zhu, B. Cui, The structure property and adsorption capacity of new enzyme-treated potato and sweet potato starches, Int. J. Biol. Macromol. 144 (2020) 863–873.
[14] H.Y. Zhang, L.J. Chen, J.B. Li, M.S. Lu, L.J. Han, Quantitative characterization of enzyme adsorption and hydrolytic performance for ultrafine grinding pretreated corn stover, Bioresour. Technol. 234 (2017) 23–32.
[15] Y. Zou, Y.Y. Ding, W.W. Feng, W. Wang, Q. Li, Y. Chen, H.Y. Wu, X.Y. Wang, L.Q. Yang, X.Y. Wu, Enzymolysis kinetics, thermodynamics and model of porcine cerebralprotein with single-frequency countercurrent and pulsed ultrasound-assisted processing, Ultrason. Sonochem. 28 (2016) 294–301.
[16] B. Wang, T.T. Meng, H.L. Ma, Y.Y. Zhang, Y.L. Li, J. Jin, X.F. Ye, Mechanism study of dual-frequency ultrasound assisted enzymolysison rapeseed protein by immobilized Alcalase, Ultrason. Sonochem. 32 (2016) 307–313.
[17] A.L. Prajapat, P.B. Subhedar, P.R. Gogate, Ultrasound assisted enzymatic depolymerization of aqueous guar gum solution, Ultrason. Sonochem. 29 (2016) 84–92.
[18] F.R. Hou, X.B. Ma, L.H. Fan, D.L. Wang, T. Ding, X.Q. Ye, D.H. Liu, Enhancement of chitin suspension hydrolysis by a combination of ultrasound and chitinase, Carbohydr. Polym. 231 (2020) 115669.
[19] B.A. Bhanvase, A. Veer, S.R. Shirsath, S.H. Sonawane, Ultrasound assisted preparation, characterization and adsorption study of ternary chitosan-ZnO-TiO_2 nanocomposite: Advantage over conventional method, Ultrason. Sonochem. 52 (2019) 120–130.
[20] L.B.L. Lim, N. Priyantha, D.T.B. Tennakoon, H.I. Chieng, M.K. Dahri, M. Suklueng, Breadnut peel as a highly effective low-cost biosorbent for methylene blue: Equilibrium, thermodynamic and kinetic studies, Arab. J. Chem. 10 (2017) S3216–S3228.
[21] K.Y. Foo, B.H. Hameed, Insights into the modeling of adsorption isotherm systems, Rev Chem Eng J. 156 (2010) 2–10.
[22] J. Zolgharnein, N. Asanjarani, S.N. Mousavi, Optimization and characterization of Tl(I) adsorption onto modified *Ulmus carpinifolia* tree leaves, Clean: Soil, Air, Water 39 (2010) 250–258.
[23] M. He, C. Chang, N. Peng, L.N. Zhang, Structure and properties of hydroxyapatite/cellulose nanocomposite films, Carbohydr Polym. 87 (2012) 2512–2518.
[24] R.L. Tseng, P.H. Wu, F.C. Wu, R.S. Juang, A convenient method to determine kinetic parameters of adsorption processes by nonlinear regression of pseudo-nth-order equation, Chem Eng J. 237 (2014) 153–161.
[25] D. Mitrogiannis, G. Markou, A. Çelekli, H. Bozkurt, Biosorption of methylene blue onto *Arthrospira platensis* biomass: Kinetic, equilibrium and thermodynamic studies, J. Environ. Chem. Eng. 3 (2015) 670–680.
[26] M. Auta, B.H. Hameed, Chitosan–clay composite as highly effective and low-cost adsorbent for batch and fixed-bed adsorption of methylene blue, Chem. Eng. J. 237 (2014) 352–361.
[27] J.A. González, M.E. Villanueva, L.L. Piehl, G.J. Copello, Development of a chitin/graphene oxide hybrid composite for the removal of pollutant dyes: adsorption and desorption study, Chem. Eng. J. 280 (2015) 41–48.
[28] Z. Aksu, S. Tezer, Biosorption of reactive dyes on the green alga *Chlorella vulgaris*, Process Biochem. 40 (2005) 1347–1361.
[29] D.K. Mahmoud, M.A.M. Salleh, W.A.W.A. Karim, A. Idris, Z.Z. Abidin, Batch adsorption of basic dye using acid treated kenaf fibre char: equilibrium, kinetic and thermodynamic studies, Chem. Eng. J. 181–182 (2012) 449–457.
[30] B. Sajjadi, J.W. Broome, W.Y. Chen, D.L. Mattern, N.O. Egiebor, N. Hammer, C.L. Smith, Urea functionalization of ultrasound-treated biochar: A feasible strategy for enhancing heavy metal adsorption capacity, Ultrason. Sonochem. 51 (2019) 20–30.
[31] M.S. Derakhshan, O. Moradi, The study of thermodynamics and kinetics methyl orange and malachite green by SWCNTs, SWCNT-COOH and SWCNT-NH_2 as adsorbents from aqueous solution, J. Ind. Eng. Chem. 20 (2014) 3186–3194.
[32] R. Nodehi, H. Shayesteh, A.R. Kelishami, Enhanced adsorption of congo red using cationic surfactant functionalized zeolite particles, Microchem. J. 153 (2020) 104281.
[33] A. Dbik, S. Bentahar, M.E.I. Khomri, N.E.I. Messaoudi, A. Lacherai, Adsorption of Congo red dye from aqueous solutions using tunics of the corm of the saffron, Mater. Today: Proc. 22 (2020) 134–139.
[34] S. Chatterjee, S. Chatterjee, B.P. Chatterjee, A.K. Guha, Adsorptive removal of congo red, a carcinogenic textile dye by chitosan hydrobeads: Binding mechanism, equilibrium and kinetics, Colloids Surf., A: Physicochem. Eng. Aspects 299 (2007) 146–152.
[35] V.J.P. Vilar, C.M.S. Botelho, R.A.R. Boaventura, Methylene blue adsorption by algal biomass-based materials: biosorbents characterization and process behavior, J. Hazard. Mater. 147 (2007) 120–132.
[36] S. Nethaji, A. Sivasamy, A.B. Mandal, Preparation and characterization of corn cob activated carbon coated with nano-sized magnetite particles for the removal of Cr (VI), Bioresour. Technol. 134 (2013) 94–100.
[37] C.Y. Wei, Y. Huang, Q. Liao, A. Xia, X. Zhu, X.Q. Zhu, Adsorption thermodynamic characteristics of *Chlorella vulgaris* with organic polymer adsorbent cationic starch: Effect of temperature on adsorption capacity and rate, Bioresour. Technol. 293 (2019) 122056.
[38] R. Kumar, M.A. Barakat, Decolourization of hazardous brilliant green from aqueous solution using binary oxidized cactus fruit peel, Chem. Eng. J. 226 (2013) 377–383.
[39] R. Lafi, K. Charradi, M.A. Djebbi, A. Ben Haj Amara, A. Hafiane, Adsorption study of Congo red dye from aqueous solution to Mg-Al-layered double hydroxide, Adv. Powder Technol. 27 (2016) 232–237.
[40] B. Acemioğlu, Adsorption of congo red from aqueous solution onto calcium-rich fly ash, J. Colloid Interface Sci. 274 (2004) 371–379.
[41] J.N.I. Balitaan, J.M. Yeh, K.S. Santiago, Marine waste to a functional biomaterial: Green facile synthesis of modified-β-chitin from *Uroteuthis duvauceli* pens (gladius), International Int. J. Biol. Macromol. 154 (2020) 1565–1575.
[42] A.E.S. Choi, S. Roces, N. Dugos, A. Arcega, M.W. Wan, Adsorptive removal of dibenzothiophene sulfone from fuel oil using clay material adsorbents, J. Cleaner Prod. 161 (2017) 267–276.
[43] A. Deb, M. Kanmani, A. Debnath, K.L. Bhowmik, B. Saha, Ultrasonic assisted enhanced adsorption of methyl orange dye onto polyaniline impregnated zinc oxide nanoparticles: Kinetic, isotherm and optimization of process parameters, Ultrason. Sonochem. 54 (2019) 290–301.
[44] L. Guo, B. Duan, L. Zhang, Construction of controllable size silver nanoparticles immobilized on nanofibers of chitin microspheres via green pathway, Nano Res. 9 (2016) 2149–2161.
[45] X.D. Liu, J.F. Tian, Y.Y. Li, N.F. Sun, S. Mi, Y. Xie, Z.Y. Chen, Enhanced dyes adsorption from wastewater via Fe_3O_4 nanoparticles functionalized activated carbon, J. Hazard. Mater. 373 (2019) 397–407.